Acta Crystallographica Section D
Biological Crystallography
ISSN 0907-4449

Polymorphism of microcrystalline urate oxidase from *Aspergillus flavus*

Ines Collings,[a] Yves Watier,[a] Marion Giffard,[b]* Sotonye Dagogo,[a] Richard Kahn,[c] Francoise Bonneté,[b] Jonathan P. Wright,[a] Andrew N. Fitch[a] and Irene Margiolaki[a,d]*

[a]European Synchrotron Radiation Facility, BP-220, F-38043 Grenoble CEDEX 9, France, [b]Centre Interdisciplinaire de Nanoscience de Marseille, CINaM–CNRS UPR 3118, Aix-Marseille Université, Parc Technologique et Scientifique de Luminy, Case 913,13288 Marseille CEDEX 09, France, [c]Institut de Biologie Structurale, F-38027 Grenoble CEDEX 1, France, and [d]Department of Biology, Section of Genetics, Cell Biology and Development, University of Patras, Greece

Correspondence e-mail: marion.giffard@gmail.com, irene.margiolaki@esrf.fr

Received 29 October 2009
Accepted 9 February 2010

Different polymorphs of rasburicase, a recombinant urate oxidase enzyme (Uox) from *Aspergillus flavus*, were obtained as a series of polycrystalline precipitates. Different crystallization protocols were followed in which the salt type, pH and polyethylene glycol 8000 (PEG 8000) concentration were varied. The related crystalline phases were characterized by means of high-resolution synchrotron X-ray powder diffraction. In all cases, Uox complexed with the inhibitor 8-azaxanthine (AZA) was not altered from its robust orthorhombic *I*222 phase by variation of any of the factors listed above. However, in the absence of AZA during crystallization ligand-free Uox was significantly affected by the type of salt, resulting in different crystal forms for the four salts tested: sodium chloride, potassium chloride, ammonium chloride and ammonium sulfate. Remarkable alterations of some of these phases were observed upon gradual increase of the exposure time of the sample to the synchrotron beam in addition to variation of the PEG 8000 concentration. When Uox was crystallized in Tris buffer or pure water in the absence of salt, a distinct polymorph of orthorhombic symmetry ($P2_12_12$) was obtained that was associated with significantly altered lattice dimensions in comparison to a previously reported isosymmetrical structure. The latter form of Uox exhibits enhanced stability to variation of pH and PEG 8000 concentration accompanied by minor modifications of the unit-cell dimensions in the ranges under study. Accurate lattice parameters were extracted for all crystalline phases. This study reveals the rich phase diagram of Uox, a protein of high pharmaceutical importance, which is associated with an enhanced degree of polymorphism. The outcome of our analysis verifies previously reported results as well as demonstrating polymorphs that have altered unit-cell dimensions with respect to known structural models.

1. Introduction

Uox, a homotetrameric enzyme of 135 kDa with a subunit consisting of 301 amino acids, is responsible for the first step in the degradation of uric acid to allantoin. It is found in a variety of organisms, but its expression is absent in humans and many primates owing to several precise mutations and deletions (Wu *et al.*, 1992). These mutations may have been conserved during evolution, as uric acid has antioxidant properties that protect the body against neurological degenerative diseases and age-related cancers (Ames *et al.*, 1981). Nevertheless, accumulation of uric acid can lead to acute hyperuricaemia and gout. Consequently, Uox can be used as a protein-based drug (McGrath & Walsh, 2005), for example as Fasturtec, which is a recombinant Uox enzyme (rasburicase) that is produced by

a genetically modified *Saccharomyces cerevisiae* strain. It is prescribed to prevent renal failure arising from rapid tumour lysis or shrinkage in patients initiating chemotherapy. Impurities that are introduced during the preparation of drugs can lead to immunogenicity and hypersensitivity (Cammalleri & Malaguarnera, 2007). The use of rasburicase has drastically decreased the impurity content. To date, rasburicase has been purified using multiple steps of chromatography (McGrath & Walsh, 2005).

Crystallization may be employed in order to formulate a protein drug (Yang *et al.*, 2003; Basu *et al.*, 2004). Protein crystals have better stability than proteins in solution for storage and have a limited manufacturing cost compared with lyophilization. Moreover, this method allows a highly concentrated formulation with a limited viscosity with respect to liquid formulations, which makes drug handling easier. Finally, it confers more sustained release of the drug compared with a liquid formulation, as the crystals progressively dissolve in the body. However, to date insulin is the only such drug that is available in a crystalline form (Havelund, 2009; Brader & Sukumar, 2005). This limitation arises from the general difficulty of obtaining protein crystals and concurrently meeting pharmaceutical requirements. In effect, the production of small isogranular and isometric crystals (10 µm) is necessary to facilitate the formulation of an injectable drug. The crystal supernatant must only contain additives that are approved as nontoxic and that are present at a physiological osmolality (equivalent to a total NaCl concentration of 130 m*M*, which may be insufficient for protein crystallization). Furthermore, two parameters theoretically control drug release from a crystal: the protein size and polymorphism. As most proteins have good solubility in physiological solution, there is a requirement to decrease the drug-release rate. This could be enabled by the use of larger crystals. Crystal size control can be achieved by variation of the concentration of the crystallizing agent (with a consequent decrease in supersaturation and nucleation rate) and *via* seeding. However, the size of the crystals has to be smaller than 50 µm in order for them to be easily injectable and to limit possible immunogenicity reactions (Rabinow, 2004). As polymorphism and crystal packing govern crystal solubility, this is a second way to affect the drug-release rate and thus the bioavailability. The latter method can have a dramatic effect on the commercialization of a drug (Aguiar *et al.*, 1967; Bauer *et al.*, 2001). The polymorphism of the crystals has to be fully characterized in order to formulate a drug in solid form; this is mandatory for the drug's submission to the Health Authorities. Powder diffraction is in this case the most suitable tool for the characterization of different polymorphs as it provides information on numerous microcrystalline samples. Additionally, it has been reported that the crystal habit itself can play a role in the release of a protein drug (Pechenov *et al.*, 2004).

Powder diffraction has recently been employed to investigate small protein structures (VonDreele, 2003; Margiolaki *et al.*, 2007; Margiolaki & Wright, 2008). The inevitable loss of information arising from the collapse of three-dimensional reciprocal space into a one-dimensional powder diffraction pattern is an obvious disadvantage with respect to single-crystal diffraction. Nevertheless, the powder technique provides complementary information which may be more difficult to obtain *via* single-crystal diffraction. The peak shapes depend on the microstructure of the material and accurate unit-cell parameters can be obtained more easily from the high angular resolution data (the angular resolution is at least an order of magnitude better than that obtained in a typical single-crystal experiment using an area detector). Moreover, as demonstrated in this paper, polycrystalline precipitates can be obtained and studied under a wide variety of crystallization conditions which may be inaccessible in soaking or single-crystal growth experiments.

2. Materials and methods

2.1. Crystallization

Recombinant Uox (rasburicase) from *Aspergillus flavus* expressed in *Saccharomyces cerevisiae* was supplied by Sanofi–Aventis without inhibitor in a phosphate buffer. Rasburicase was placed in the relevant buffer (50 m*M* Tris buffer pH 7.0–9.0 or water) using gel-filtration chromatography on Superdex S200PG with an ÄKTA Basic system. The pH of the Tris buffer was adjusted with HCl prior to protein transfer. The pH of the buffer solution was found to remain unaffected when the protein was introduced. 8-Azaxanthine (Sigma–Aldrich) was incubated with the rasburicase solution when necessary and any excess was removed using gel-filtration chromatography as described above. The rasburicase stock solution was kept at 3 mg ml^{-1} in a cold room and was concentrated when needed.

Crystallization of a 3 mg ml^{-1} rasburicase solution without salt (Tris buffer or water) took place in approximately a week at 283 K. The addition of PEG 8000 to a concentration of greater than 2% at room temperature resulted in a reduced crystallization time. At a later stage, it was observed that keeping the solutions in a cold room (277 K) for approximately two weeks before data collection led to better diffraction quality, possibly owing to enhanced crystallinity of the protein precipitants.

According to previous observations (Giffard *et al.*, 2008), the addition of salt at a concentration of between 10 m*M* and 1 *M* induces the dissolution of pre-existing rasburicase crystals or may prevent its crystallization. Addition of PEG 8000 to the solution counterbalances this effect and induces the growth of crystals in solutions of rasburicase containing salt.

1 *M* stock solutions of NaCl, KCl, NH_4Cl and $(NH_4)_2SO_4$ (Sigma–Aldrich) were prepared by dilution of the appropriate amounts of salt in 50 m*M* Tris buffer pH 8.0. A solution of 40%(*w*/*v*) PEG 8000 in 50 m*M* Tris buffer pH 8.0 was prepared from a 50%(*w*/*v*) solution (Hampton Research). All salt and rasburicase solutions for crystallization trials were filtered through 0.22 µm Millipore filters. All crystallization experiments were performed using the batch method and the microcrystals obtained corresponding to different crystal forms are presented in Fig. 1.

2.2. X-ray data collection and processing

Powder X-ray diffraction data were collected at room temperature with a wavelength of 1.30000 (6) Å using the high-resolution powder diffraction beamline ID31 at ESRF, Grenoble (Fitch, 2004). The nine analyser crystals which are separated by ∼2° were scanned over a 20° 2θ range in 1–3 min with a sampling time of 3 ms. All samples were loaded into 1 mm diameter borosilicate glass capillaries and centrifuged in order to enhance crystal packing. Excess mother liquor was removed and the capillaries were sealed with wax to prevent dehydration. The capillaries were mounted on the diffractometer and spun at high speed (1000 rev min^{-1}) to ensure adequate powder averaging and therefore reduce the effect of any preferred orientation of the polycrystalline sample. Hence, samples were mounted on a fast capillary spinner which also allows the sample to be translated along the axis of the diffractometer. An automatic sample-changing robot was used for loading and unloading all the samples by mounting the capillaries in self-centring magnetic bases. Several scans were collected per sample position, with the capillaries being translated periodically to expose a fresh region of sample that was unaffected by the synchrotron beam. Radiation-damage effects are accompanied by marked changes in lattice parameters along with gradual increases in peak broadening and can be monitored by comparing the profile measured in each of the nine channels during a single scan, as well as by comparing subsequent scans. The first scans, where the sample had just been translated to expose fresh material, were combined, leading to increased counting statistics without compromising the data quality for structure analysis, while the subsequent scans showed detectable degradation and were only employed to follow the evolution of cell dimensions with increasing exposure time. In most cases, profiles were collected with a period of 1.0 min owing to rapid radiation damage, using a beam size of 1.5 × 1.0 mm. Samples of the orthorhombic phase (space group *I*222) of Uox complexed with its inhibitor 8-azaxanthine (AZA) exhibited a longer lifetime in the synchrotron beam and therefore data were collected with a period of 3.0 min. In the case of Uox crystallized with NH_4Cl or KCl, anisotropic lattice-parameter evolution was observed after only 15 s of exposure to the beam owing to radiation damage. For this special case, profiles were added in 15 s time windows for each scan in order to follow this effect more closely.

3. Le Bail analysis for the extraction of precise lattice parameters

Using 2θ positions extracted from at least the first 20 diffraction peaks present in the collected profiles, all patterns were indexed using the *TOPAS*-4 program (Bruker AXS; see Table 1 for more details). Throughout this study, we identified various crystal forms involving five different space groups which are described in the following sections. The microcrystals obtained under different crystallization conditions are shown in Fig. 1. All forms conserve the same basic molecular tetramers; however, the different ways in which these are

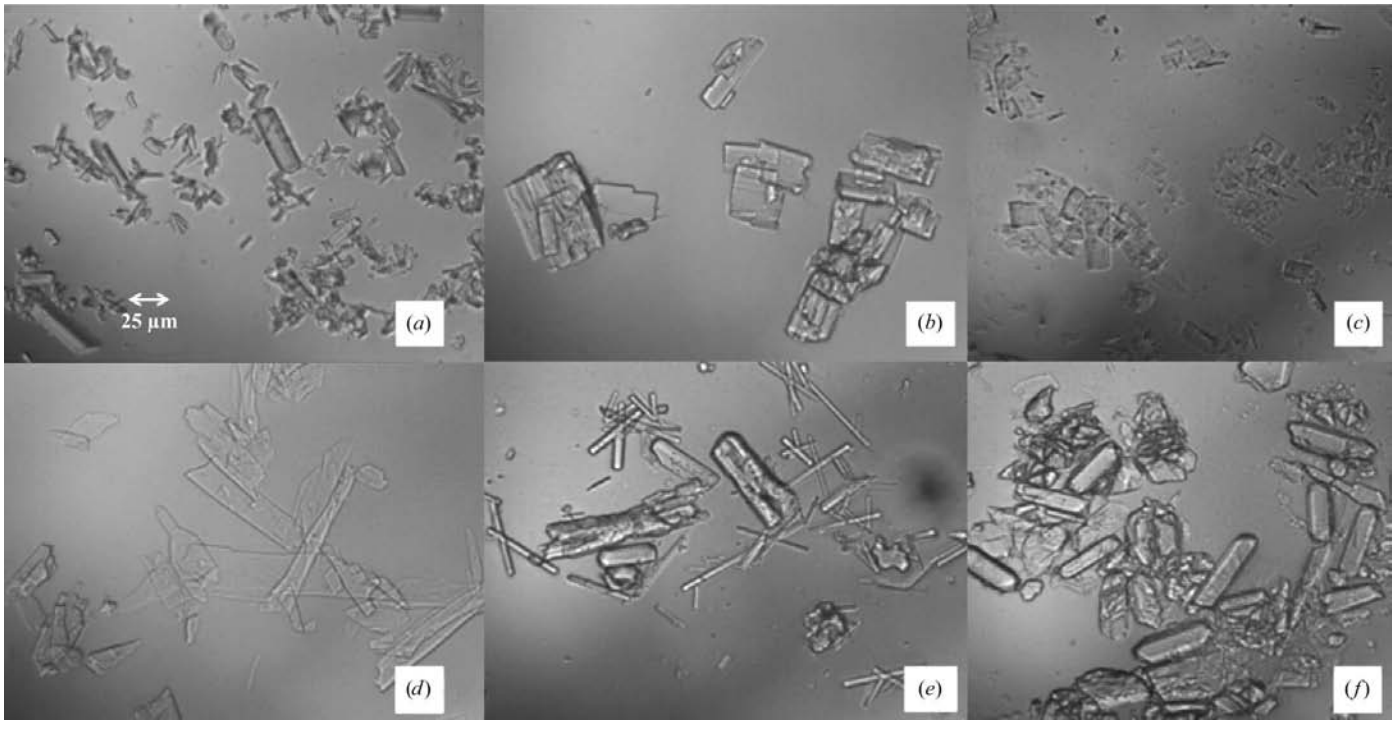

Figure 1
Optical microscopy images of Uox microcrystals prepared under different conditions. (*a*) Ligand-free Uox with NH_4Cl and 15% PEG 8000, (*b*) ligand-free Uox with NaCl and 15% PEG 8000, (*c*) ligand-free Uox with $(NH_4)_2SO_4$ and 15% PEG 8000, (*d*) ligand-free Uox with 10% PEG, (*e*) ligand-free Uox with KCl and 10% PEG 8000, (*f*) Uox complexed to AZA with NaCl and 10% PEG 8000.

Table 1
Details of sample crystallization, data collection and Le Bail analysis (Le Bail *et al.*, 1988) of the powder profiles.

Uox crystallized with	NH_4Cl	NaCl	NaCl	$(NH_4)_2SO_4$	H_2O	KCl	Complexed AZA
PEG concentration (%)	15	15	8	15	15	10	10
Data collection							
Wavelength (Å)	1.30000 (6)	1.30000 (6)	1.53986 (6)	1.30000 (6)	1.30000 (6)	1.30000 (6)	1.30000 (4)
Exposure time per scan (s)	60	60	60	60	60	60	180
LeBail refinement							
Space group	$P3_121$	$P2_1$	$P2_1$	$P2_1$	$P2_12_12$	$P3_121$	$I222$
Unit-cell parameters							
a (Å)	140.4002 (9)	81.8712 (9)	82.593 (2)	75.4153 (8)	133.6473 (19)	141.455 (3)	80.2944 (3)
b (Å)	140.4002 (9)	124.7628 (13)	141.723 (4)	141.8930 (15)	135.9379 (16)	141.455 (3)	96.2244 (3)
c (Å)	151.1053 (13)	142.9454 (15)	134.919 (3)	149.5638 (15)	78.9043 (9)	151.273 (5)	105.5280 (3)
α (°)	90	90	90	90	90	90	90
β (°)	90	93.7280 (6)	92.714 (14)	94.4041 (6)	90	90	90
γ (°)	120	90	90	90	90	120	90
Volume (Å^3)	2579560 (40)	1457020 (30)	1577490 (70)	1595740 (30)	1433510 (30)	2621400 (100)	815340 (5)
Matthews coefficient (Å^3 Da^{-1})	3.14	2.66	2.88	2.90	2.60	3.19	2.95
Solvent content (%)	60.8	53.8	57.3	57.6	52.7	61.4	58.3
No. of monomers per ASU	4	8	8	8	4	4	1
Resolution range (Å)	121.6–8.0	142.6–10.0	134.8–12.0	149.0–10.0	95.3–8.2	121.5–7.5	106.4–3.6

packed in the corresponding unit cells distinguish the phases observed.

3.1. Orthorhombic ($P2_12_12$) phase

In the absence of salt, in Tris buffer or pure water, PEG 8000 is not essential for crystallization. The low protein solubility makes Uox crystallization possible in the absence of precipitant agents. Ligand-free Uox crystallized in pure water or Tris buffer adopts an orthorhombic symmetry (space group $P2_12_12$) comprising one protein tetramer per asymmetric unit (ASU). This phase has been studied in detail owing to its relevance to the Uox salting-in effect (Giffard *et al.*, 2008). In order to obtain exact values of the unit-cell parameters, unit-cell refinement *via* the Le Bail method was employed (Le Bail *et al.*, 1988) using the *TOPAS*-4 software (Bruker AXS).

In addition, the effects of pH (from 7.0 to 9.0 in Tris buffer) and PEG 8000 concentration (up to 16%) were studied. The microcrystals obtained at different pH values are shown in Fig. 2. Both factors resulted in minor alterations of the unit-cell dimensions. pH variation (from 7.2 to 9.0) resulted in a decrease of the unit-cell volume of $\Delta V/V_i = (V_f - V_i)/V_i = -0.04\%$ at 0% PEG 8000 and an increase of $\Delta V/V_i = 0.05\%$ at 8% PEG 8000 in the pH range 7.5–8.5. When the concentra-

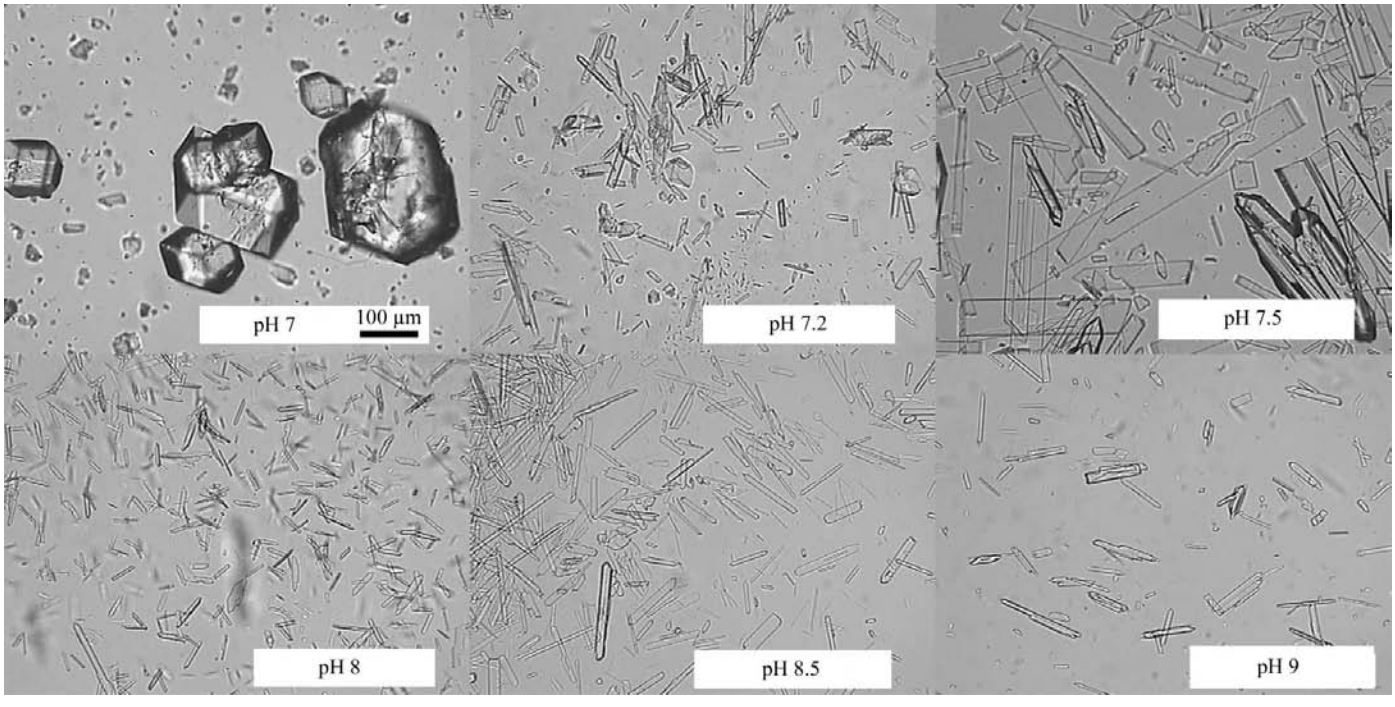

Figure 2
Optical microscopy images of microcrystalline ligand-free Uox prepared in Tris buffer at different pH values (space group $P2_12_12$).

tion of PEG 8000 was increased to 16%, a more prominent volume decrease of $\Delta V/V_i = -2.80\%$ was observed between pH 7.5 and 8.5. The evolution with pH of the refined lattice parameters for 0%, 8% and 16% PEG 8000 concentrations is presented in Fig. 3.

We investigated the effect of precipitant concentration on this phase by varying the PEG 8000 concentration from 0% to 24% at pH 8.0. For PEG 8000 concentrations lower than 16% we did not observe any marked modifications of the orthorhombic lattice parameters as shown in Fig. 4 ($\Delta V/V_i = -0.58\%$ from 0% to 16% PEG 8000 concentration). Upon further increase of the PEG 8000 concentration to 24% we observed an abrupt drop in the unit-cell volume ($\Delta V/V_i = -7.00\%$ from 0% to 24% PEG 8000 concentration) while conserving the orthorhombic symmetry.

The lattice parameters of this phase did not match those of any similar model available from the PDB. Nevertheless, the 1xxj model (Retailleau *et al.*, 2005; Uox complexed with 5-amino 6-nitrouracil) with space group $P2_12_12$ was used for molecular replacement. However, with such a large protein and the limited data resolution of the measured profiles (8.2 Å) no clear solution could be distinguished in the list of tentative solutions. Improved data quality is required in order to resolve this structure.

3.2. Trigonal ($P3_121$) phase

When we followed a different crystallization route, employing NH_4Cl or KCl in the presence of PEG 8000 at pH 8.0, ligand-free Uox crystallized in a phase with trigonal symmetry (space group $P3_121$) containing one protein tetramer per ASU. This phase has the largest unit-cell volume and the highest solvent content (61%) of all the Uox polymorphs reported in this study.

In both conditions (NH_4Cl and KCl) an unexpected anisotropic lattice-parameter evolution was observed with increasing exposure time of the sample to the synchrotron beam. In the case of Uox crystallized with NH_4Cl the *c* crystallographic axis decreased abruptly ($\Delta c/c_i = -1.16\%$) between 45 and 75 s exposure time, whereas the *a* axis did not evolve in the same manner ($\Delta a/a_i = 0.39\%$). The refined lattice parameters are shown in Fig. 5.

In the case of Uox crystallized with KCl we observed a similar anisotropic lattice-parameter evolution with increasing exposure irradiation time, imitating a second-order phase transition. A lattice-parameter decrease along the *c* axis was detected ($\Delta c/c_i = -1.22\%$), whereas the *a* axis did not show a significant evolution ($\Delta a/a_i = 0.11\%$) between 15 and 75 s exposure time.

The extracted lattice parameters are closely related to the PDB models of Uox complexed with uracil (1ws3) and 5,6-diaminouracil (1ws2) listed in Table 2 (Retailleau *et al.*, 2005). However, even with these starting models the data quality (8 Å) was insufficient for solving the structure *via* MR.

3.3. Monoclinic ($P2_1$) phases

In the presence of NaCl or $(NH_4)_2SO_4$ during crystallization Uox formed crystals of monoclinic symmetry (space group $P2_1$) with two Uox tetramers in the asymmetric unit. When Uox was crystallized with $(NH_4)_2SO_4$ the unit-cell volume was larger by 8.7% than that of the phase obtained with NaCl (Table 1).

In the case where NaCl was employed during crystallization of ligand-free Uox with 8% PEG 8000, a monoclinic phase was observed which corresponds to the previously published $P2_1$ ligand-free phase (Retailleau *et al.*, 2005). Uox crystallized with NaCl is strongly affected by the PEG 8000 concentration, the duration of crystallization and radiation damage. Specifi-

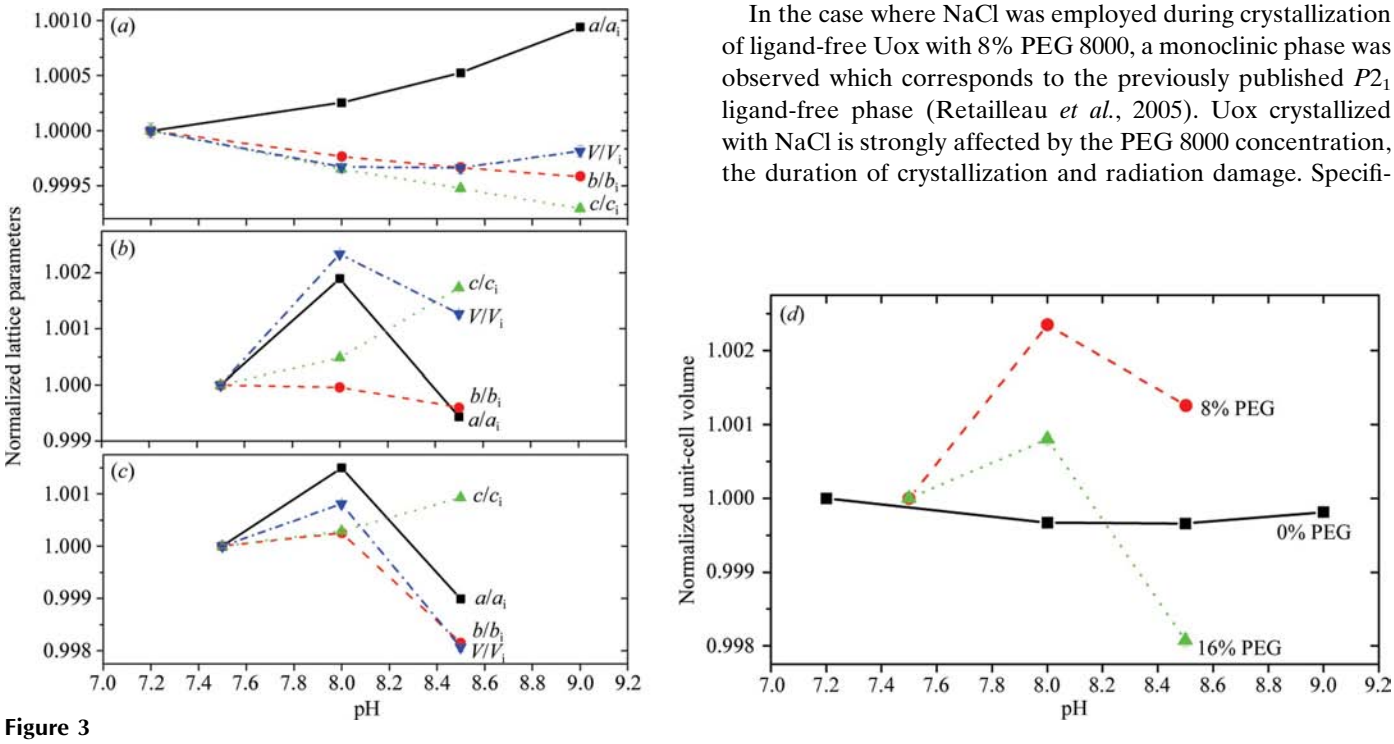

Figure 3
pH evolution of the normalized lattice parameters and unit-cell volume of orthorhombic ($P2_12_12$) ligand-free Uox crystallized in Tris buffer without salt using (*a*) 0% PEG, (*b*) 8% PEG and (*c*) 16% PEG. (*d*) shows the pH evolution of the normalized unit-cell volume of all three Uox forms listed above.

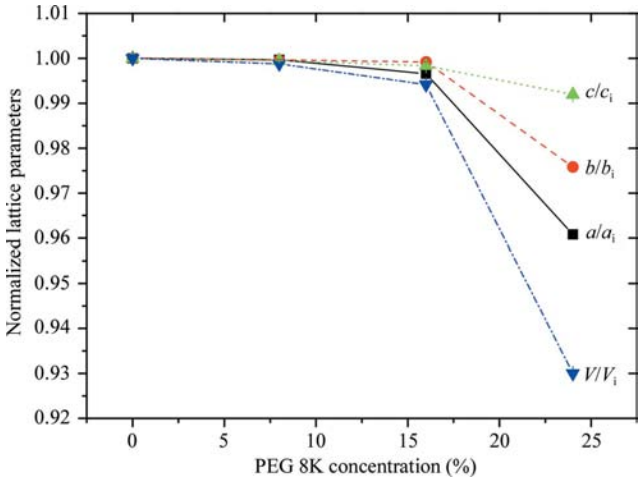

Figure 4
Evolution of the normalized lattice parameters of orthorhombic ($P2_12_12$) ligand-free Uox crystallized in Tris buffer without salt at pH 8 with increasing PEG 8000 concentration.

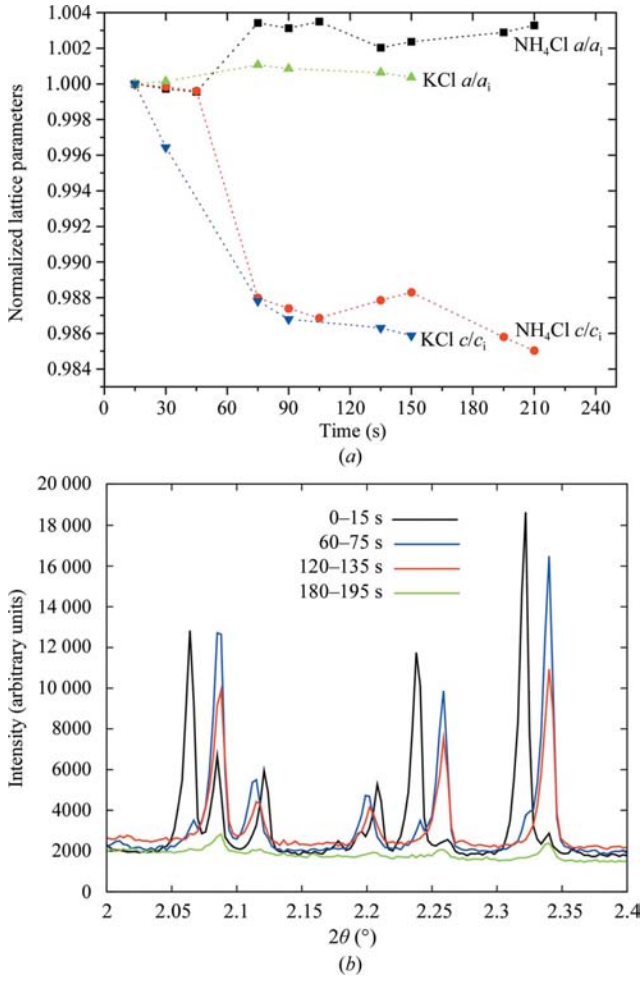

Figure 5
(*a*) Anisotropic variation of the normalized lattice dimensions of trigonal ligand-free Uox crystallized with NH_4Cl or KCl at pH 8 ($P3_121$) with increasing sample exposure time to the synchrotron beam. (*b*) Selected 2θ regions of powder diffraction profiles of Uox crystallized with NH_4Cl at pH 8 [ID31; $\lambda = 1.30000$ (6) Å, 295 K] showing a gradual evolution of the peak positions and widths with increasing irradiation time. The colours correspond to different sample exposure times varying from 15 to 195 s.

Table 2
Different structural models of Uox available in the PDB related to the phases reported in this study.

All crystallization was performed in the presence of 5–8%(*w*/*v*) PEG 8000 at pH 8.5 with the inhibitors added in large excess.

Uox	1ws3	1xy3	1xxj	1r51
Ligand	Uracil	Guanine	Benzene	8-Azaxanthine
Space group	$P3_121$	$P2_1$	$P2_12_12$	$I222$
Unit-cell parameters				
a (Å)	140.60	82.75	126.25	81.30
b (Å)	140.60	141.94	142.27	96.30
c (Å)	151.08	135.08	81.32	105.60
α (°)	90	90	90	90
β (°)	90	92.67	90	90
γ (°)	120	90	90	90
Matthews coefficient (Å^3 Da^{-1})	3.14	2.66	2.60	2.95
Solvent content (%)	60.8	53.8	52.7	58.3
No. of monomers per ASU	4	8	4	1

cally, upon a gradual increase of the PEG 8000 concentration from 8% to 10% and 15% initial measurements indicated a major change in the powder profiles, as shown in Fig. 6. This effect has been interpreted in terms of a continuous phase change accompanied by a distinct modification of the cell dimensions (see Table 1). At 10% PEG 8000 we observed the coexistence of the 8% and 15% PEG 8000 monoclinic phases. We have initiated a systematic investigation in order to disentangle the effects of the duration of crystallization and

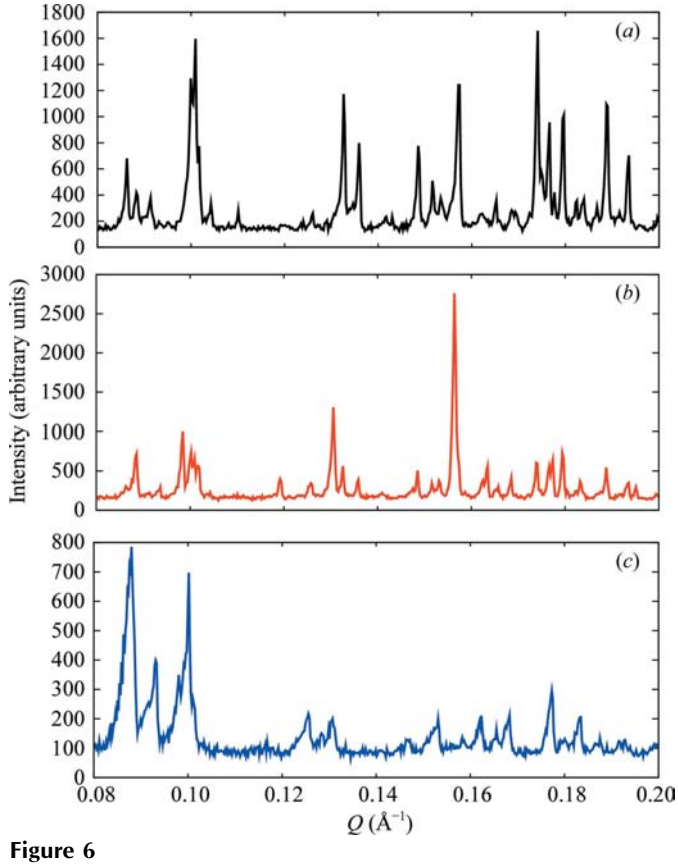

Figure 6
Selected Q-region of diffraction profiles of ligand-free Uox crystallized with NaCl at pH 8 and (*a*) 8% PEG 8000, (*b*) 10% PEG 8000 and (*c*) 15% PEG 8000.

PEG 8000 concentration and the results will be reported elsewhere.

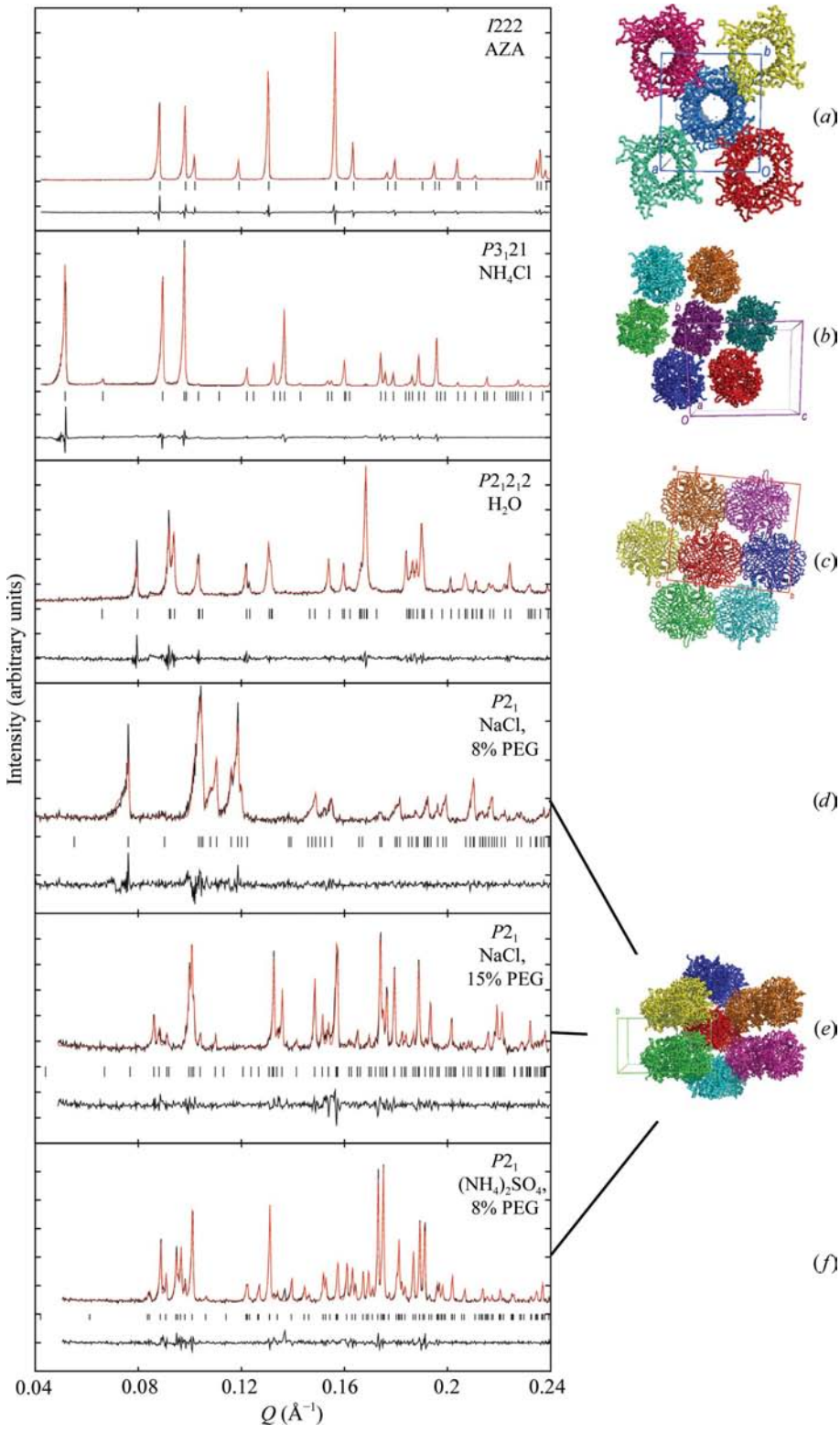

Figure 7
Left, selected Q-region of the Le Bail fits for six distinct phases of Uox reported in this study. Right, projection in the *ab* plane of candidate structure models available in the PDB: (*a*) 1r51 (Retailleau *et al.*, 2004), (*b*) 1ws3 (Retailleau *et al.*, 2005), (*c*) 1xxj (Retailleau *et al.*, 2005) and (*d*, *e*, *f*) 1xy3 (Retailleau *et al.*, 2005).

Furthermore, when $(NH_4)_2SO_4$ was employed during crystallization a monoclinic phase was obtained (space group $P2_1$) characterized by significantly different lattice dimensions with respect to the known structural model (Retailleau *et al.*, 2005).

3.4. Orthorhombic (*I*222) phase

The orthorhombic *I*222 phase was obtained upon the addition of an excess of the inhibitor 8-azaxanthine (AZA). This resulted in a robust crystal structure with no significant alterations upon variation of salt, PEG 8000 concentration or pH. The extracted unit-cell parameters are similar to those previously reported (Retailleau *et al.*, 2004) with one monomer (one quarter of a tetramer) in the ASU. Among all the forms identified in this study, this phase displayed by far the best X-ray powder diffraction data quality (Table 1) and resistance to radiation. The collected profiles can be modelled well, with a wealth of diffraction peaks extending to high angles and with excellent counting statistics. Detailed structural analysis of this crystal form of Uox will be presented in a subsequent paper (Watier *et al.*, in preparation).

4. Discussion

In the present study, we focus on the effects of salt type as well as of pH and PEG 8000 concentration on the crystal motifs of ligand-free Uox and of Uox complexed with AZA. High-resolution powder diffraction measurements have revealed seven distinct phases corresponding to five crystallographic symmetries (Table 1). When Uox was crystallized in Tris buffer or pure water in the absence of salt a distinct polymorph with orthorhombic symmetry ($P2_12_12$) was obtained that was associated with significantly altered lattice parameters in comparison to a previously reported isosymmetrical structure (PDB code 1xxj; Retailleau *et al.*, 2005). Crystallization experiments under various pH conditions and at various PEG 8000 concentrations followed by diffraction measurements employing microcrystalline protein

precipitants revealed interesting evolutions of the cell dimensions.

Specifically, ligand-free Uox in the presence of PEG 8000 at pH 8.0 was greatly affected by the salt employed for crystallization. Distinct polymorphs characterized by altered crystallographic symmetries and/or cell dimensions were obtained depending on the salt type (Table 1). Microcrystals formed under various conditions are shown in Fig. 1 and the collected profiles together with candidate structural models available in the PDB and LeBail fits to the data are shown in Figs. 7 and 8. It is known from the structure of Uox complexed with AZA that cations bind at specific locations on the surface of the protein (Giffard *et al.*, 2008). The resolution of the powder diffraction data was inadequate to verify that the same phenomenon is sustained in the case of ligand-free Uox. However, as these sites are not in the proximity of the active site where AZA is located they most probably also exist on the surface of ligand-free Uox. These surface cations could affect the way the proteins pack as well as the protein contacts in the three-dimensional network of the crystal, resulting in the salt-dependent polymorphism reported here. Moreover, in the cases in which NH_4Cl or KCl were employed for crystallization an unexpected anisotropic lattice-parameter evolution was observed with increasing sample exposure time to the synchrotron beam (Fig. 5).

In the absence of salt Uox crystallized in an orthorhombic unit cell with the smallest volume and solvent content of the identified crystal forms (Fig. 2). Further investigation of variation of the pH and PEG 8000 concentration in ligand-free Uox without salt showed minor lattice-parameter evolution within the pH range 7.0–9.0 and the PEG 8000 concentration range 0–16% (Fig. 3). At PEG 8000 concentrations as high as a 24% collapse of the unit cell was observed, with the *a* lattice parameter being affected the most (Fig. 4). This effect can be

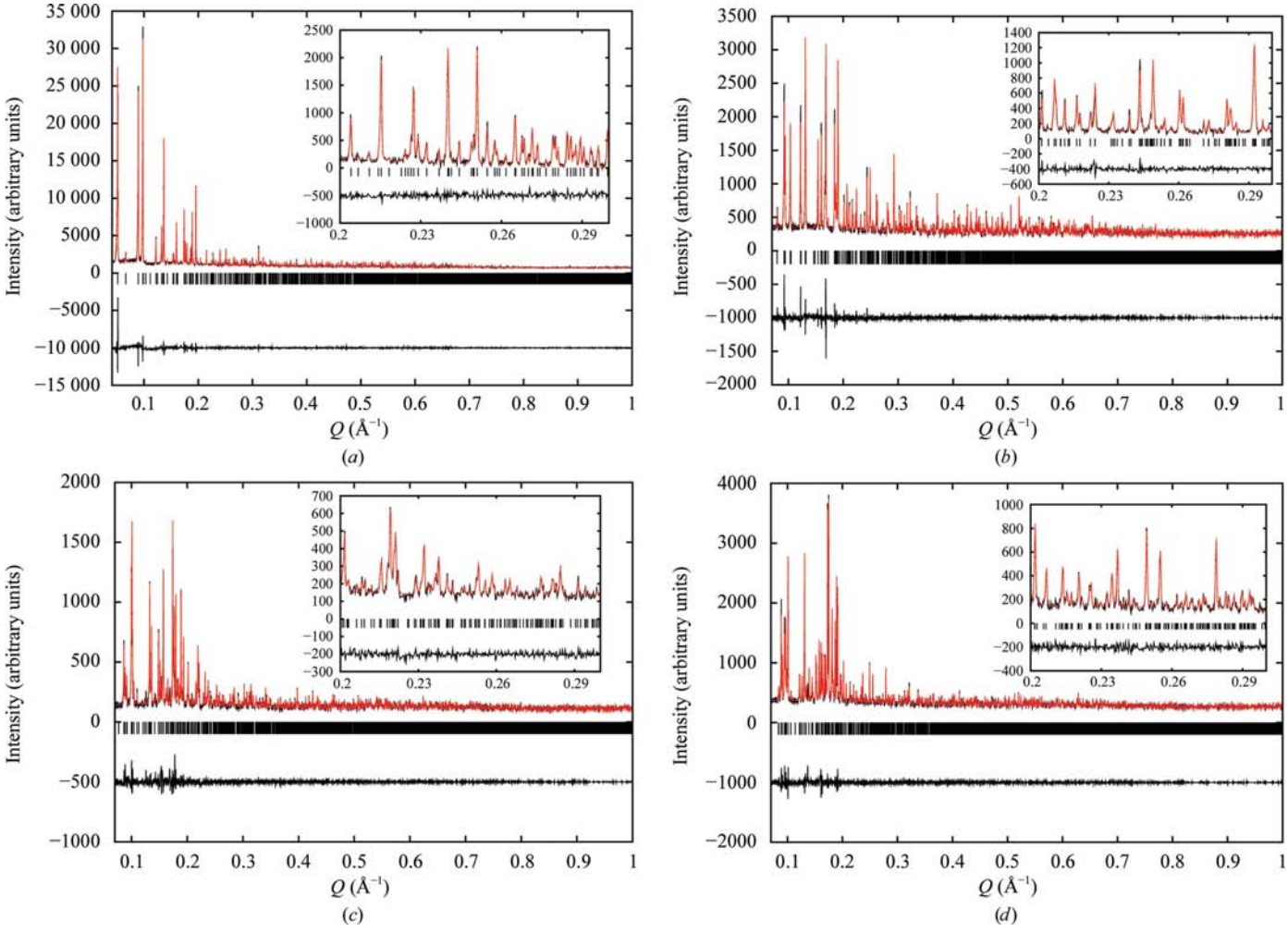

Figure 8
LeBail fits of all seven phases of Uox reported in this study [ID31; λ = 1.30000 (6) Å, 295 K]. (*a*) Ligand-free Uox crystallized with NH_4Cl and 15% PEG 8000 ($P3_121$), (*b*) ligand-free Uox crystallized in water with 10% PEG 8000 ($P2_12_12$), (*c*) ligand-free Uox crystallized with NaCl and 15% PEG 8000 ($P2_1$), (*d*) ligand-free Uox crystallized with $(NH_4)_2SO_4$ and 15% PEG 8000 ($P2_1$). The black, red and lower black lines represent the experimental data, the calculated pattern and the difference between the experimental and calculated profiles, respectively. The vertical bars correspond to Bragg reflections compatible with the particular space group. The insets correspond to magnifications of the fits in selected *Q* ranges.

interpreted in terms of the replacement or removal of water molecules by PEG 8000. However, a detailed structural study is required in order to further investigate this phenomenon.

The PEG 8000 concentration had a more pronounced effect on ligand-free Uox crystallized in NaCl at pH 8.0. An increase in the PEG 8000 concentration from 8% to 15% resulted in a significant modification of the cell dimensions that is evident in the alterations of the powder diffraction profiles (Fig. 6). There was an overall decrease in unit-cell volume going from 8% to 15% PEG 8000, while the lattice parameter *c* increases by 6% and *b* decreases by 12% (Table 1). At 10% PEG 8000 two phases coexist with lattice parameters that are comparable to those observed at 8% and 15%. This behaviour is indicative of a possible alteration of the intermolecular contacts in the unit cell. The duration of crystallization also had an impact in this case owing to the coexistence of two crystal structures (Table 1 and Fig. 6). Additional studies need to be undertaken in order to understand fully its evolution with PEG 8000 concentration, radiation damage and crystallization time.

The use of AZA is not currently relevant from the point of view of pharmaceutical development. However, this inhibitor has been used in the past at a low concentration as a stabilizer (Navolanic *et al.*, 2003) and the first structure of Uox was solved from the AZA complex (Colloc'h *et al.*, 1997). In this case, the AZA complex is interesting from a methodological point of view. The use of AZA for the crystallization of Uox improves the diffraction quality of the protein crystals, making possible the structural resolution of urate oxidase from its powder profile (Watier *et al.*, in preparation). To our knowledge this is the largest protein structure to be solved and refined from powder diffraction data. In addition, Uox complexed with AZA did not show marked changes in lattice parameters when the salt type, PEG 8000 concentration or pH were varied during crystallization. According to previous studies, the active site may have an effect on the structure. Therefore, as AZA stabilizes this site (Retailleau *et al.*, 2005) the regular contacts in the crystal are held together strongly and are unaffected by changes in the immediate environment.

In conclusion, we have observed systematic variations of the crystal forms of Uox by exploiting a variety of crystallization conditions. Further advantages that were gained from the use of microcrystalline samples and powder diffraction measurements include verification of the homogeneity and phase purity of the protein precipitants and extraction of accurate lattice parameters allowing direct observation of slight structure modifications and exploitation of radiation and sample-induced effects.

As far as drug design is concerned, Fasturtec is currently a drug that is intended for a single injection in the case of tumour lysis syndrome. In this case, a Uox lyophilisate, which is reconstituted in the hospital for intravenous injection, is suitable. In the case where regular injections are required, it would be more efficient to develop a subcutaneous formulation which allows self-administration, avoiding hospitalization. The main limitation of this approach is the high concentration

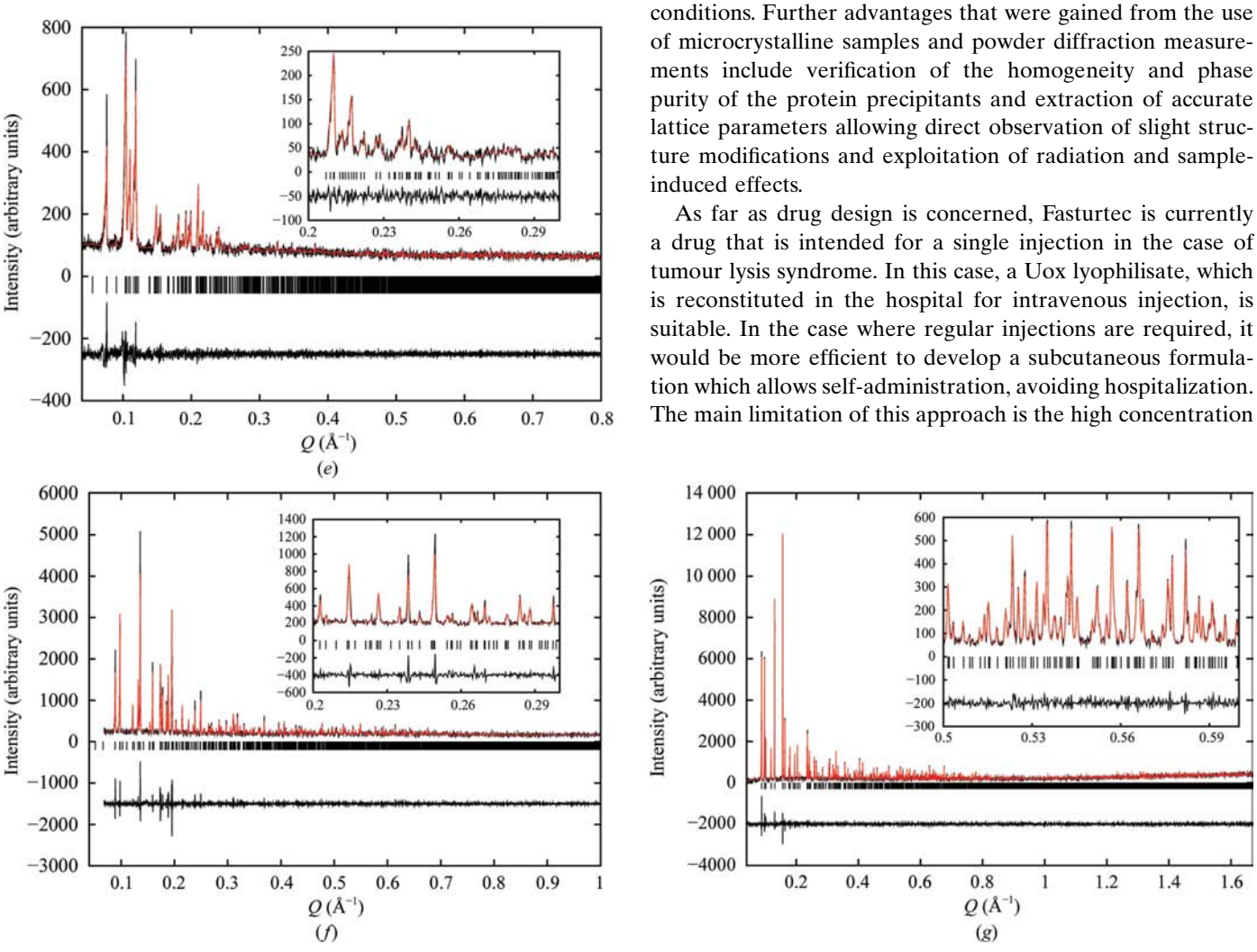

Figure 8 (continued)
LeBail fits of phases of Uox reported in this study. (*e*) Ligand-free Uox crystallized with NaCl and 8% PEG 8000 ($P2_1$), (*f*) ligand-free Uox crystallized with KCl and 10% PEG 8000 ($P3_121$), (*g*) Uox complexed with AZA and crystallized with NaCl ($I222$).

necessary to minimize the volume of the injected product. This study demonstrates the feasibility of the production and structural characterization of microcrystalline suspensions of Uox. All of the chemical components that we have employed for crystallization are acceptable for pharmaceutical use and can be used for drug formulation at isotonicity. PEG and salts may be varied to control the crystal size, shape and solubility and hence to adjust the bioavailability.

We thank the ESRF for provision of beam time on beamline ID31 and M. El-Hajji and F. Ragot from Sanofi–Aventis (France) for providing the rasburicase. We are grateful to Dr A. H. Hill for his advice and support during this project.

References

Aguiar, A. J., Krc, J. Jr, Kinkel, A. W. & Samyn, J. C. (1967). *J. Pharm. Sci.* **56**, 847–853.
Ames, B. N., Cathcart, R., Schwiers, E. & Hochstein, P. (1981). *Proc. Natl Acad. Sci. USA*, **78**, 6858–6862.
Basu, S., Govardhan, C., Jung, C. & Margolin, A. (2004). *Expert Opin. Biol. Ther.* **4**, 301–317.
Bauer, J., Spanton, S., Henry, R., Quick, J., Dziki, W., Porter, W. & Morris, J. (2001). *Pharm. Res.* **18**, 859–866.
Brader, M. L. & Sukumar, M. (2005). US Patent 2005/0054818A1.
Cammalleri, L. & Malaguarnera, M. (2007). *Int. J. Med. Sci.* **4**, 83–93.
Colloc'h, N., El Hajji, M., Bachet, B., L'Hermite, G., Schiltz, M., Prangé, T., Castro, B. & Mornon, J. P. (1997). *Nature Struct. Biol.* **4**, 947–952.
Fitch, A. N. (2004). *J. Res. Natl Inst. Stand. Technol.* **109**, 133–142.
Giffard, M., Colloc'h, N., Ferté, N., Castro, B. & Bonneté, F. (2008). *Cryst. Growth Des.* **8**, 4220–4226.
Havelund, S. (2009). US Patent 2009/0010854A9.
Le Bail, A., Duroy, H. & Fourquet, J. L. (1988). *Mater. Res. Bull.* **23**, 447–452.
Margiolaki, I. & Wright, J. P. (2008). *Acta Cryst.* A**64**, 169–180.
Margiolaki, I., Wright, J. P., Fitch, A. N., Fox, G. C., Labrador, A., Von Dreele, R. B., Miura, K., Gozzo, F., Schiltz, M., Besnard, C., Camus, F., Pattison, P., Beckers, D. & Degen, T. (2007). *Z. Kristallogr.*, Suppl. 26, 1–13.
McGrath, B. M. & Walsh, G. (2005). Editors. *Directory of Therapeutic Enzymes.* Boca Raton: CRC Press.
Navolanic, P. M., Pui, C., Larson, R. A., Bishop, M. R., Pearce, T. E., Cairo, M. S., Goldman, S. C., Jeha, S. C., Shanholtz, C. B., Leonard, J. P. & McCubrey, J. A. (2003). *Leukemia*, **17**, 499–514.
Pechenov, S., Shenoy, B., Yang, M. X., Basu, S. K. & Margolin, A. L. (2004). *J. Control. Release*, **91**, 149–158.
Rabinow, B. E. (2004). *Nature Rev. Drug Discov.* **3**, 785–796.
Retailleau, P., Colloc'h, N., Vivarès, D., Bonneté, F., Castro, B., El Hajji, M., Mornon, J.-P., Monard, G. & Prangé, T. (2004). *Acta Cryst.* D**60**, 453–462.
Retailleau, P., Colloc'h, N., Vivarès, D., Bonneté, F., Castro, B., El Hajji, M. & Prangé, T. (2005). *Acta Cryst.* D**61**, 218–229.
Von Dreele, R. B. (2003). *Methods Enzymol.* **368**, 254–267.
Wu, X., Muzny, D. M., Lee, C. C. & Caskey, C. T. (1992). *J. Mol. Evol.* **34**, 78–84.
Yang, M. X., Shenoy, B., Disttler, M., Patel, R., McGrath, M., Pechenov, S. & Margolin, A. L. (2003). *Proc. Natl Acad. Sci. USA*, **100**, 6934–6939.